Int. J. Multiphase Flow Vol. 11, No. 3, pp. 283–297, 1985
Printed in the U.S.A.

0301-9322/85 $3.00 + .00

STUDIES ON HEAT TRANSFER AND FLOW CHARACTERISTICS IN SUBCOOLED FLOW BOILING—PART 2. FLOW CHARACTERISTICS

RYUTARO HINO† and TATSUHIRO UEDA‡
Department of Mechanical Engineering, University of Tokyo, Bunkyo-ku, Tokyo 113, Japan

(*Received* 5 *June* 1984; *in revised form* 2 *October* 1984)

Abstract—Distributions of fluid temperature and its fluctuation are measured across a R-113 subcooled boiling flow channel with heat fluxes up to the CHF. A microthermocouple probe associated with an electric compensation circuit for the time constant is used for this purpose. Applying statistical treatments to the recorded temperature fluctuation, the heat transfer process in the flow and the characteristics of the bubbles flowing close to the heated surface are investigated. For high heat fluxes nearby the CHF, some bubbles adjacent to the heated surface show a clear trend to coalesce to large volume bubbles with relatively long passing periods, suggesting a mechanism of departure from nucleate boiling by periodical wall temperature rise due to momentary liquid film dryout underneath the large bubbles.

1. INTRODUCTION

In flow boiling systems, it has been known that the nucleate boiling is usually initiated at some position where the core liquid is in a subcooled state, and that the void fraction can rise to a considerably high value before the core liquid temperature reaches the saturation value. Therefore, many studies with respect to the axial distribution of void fraction in the subcooled boiling region have been done. However, the heat transfer and flow characteristics are not yet clarified in detail, since the subcooled boiling flow is in a complicated nonequilibrium state. Experimental data on the temperature distribution across the flow passage are limited. In addition, there seems to be considerable uncertainty in the literature as to the mechanism to reach the critical heat flux (CHF) condition which is of significant means for the flow boiling systems.

The purpose of this study is to investigate the boiling heat transfer characteristics, the heat transfer process and the flow state nearby the heated surface for R-113 subcooled boiling flow in a vertical concentric annulus. In the previous paper, part I (Hino & Ueda 1985), the relations between the heat flux and the wall superheat for subcooled boiling flow were examined in a range of heat fluxes from the incipient boiling to the CHF condition, comparing with the photographic observation of the flow state. In the present paper, distributions of the local fluid temperature and its fluctuation are measured across the flow passage by a microthermocouple inserted into the stream, and the flow characteristics in the process to reach the CHF condition are examined.

The fluid temperature distribution and the temperature fluctuation characteristic in the subcooled boiling flow are expected to be different from those in the single-phase liquid flow, on account of the growth and transportation of vapor bubbles and the condensation of a part of bubbles. Several experimental results of the temperature distribution for water subcooled boiling flows have been reported (Jiji & Clark 1964, Walmet & Staub 1969, Akiyama & Tachibana 1974 and Sekoguchi *et al.* 1974, 1980), but these results did not comprehend the temperature characteristics sufficiently, because the time constants of the thermocouples used in these measurements were too high to follow the temperature fluctuation accurately.

†Present address: Division of High Temperature Engineering, Japan Atomic Energy Research Institute, Tokai, Naka-Gun, Ibaragi-Prefecture, 319-11, Japan.
‡Present address: Department of Mechanical Engineering, Kogakuin University, 1, Nishishinjuku, Shinjuku-ku, Tokyo 160, Japan.

As for the pool boiling, a microthermocouple was employed to obtain the temperature fluctuation characteristic and the void fraction by Afgan (1975), and this method was tested for a subcooled boiling flow by Delhaye *et al.* (1973). However, since the temperature fluctuation in the subcooled boiling flow field of high heat fluxes involves considerably high frequency components produced by bubble flowing, a measuring technique to be able to follow up the high frequencies will be needed.

The CHF condition in the subcooled and low quality regions has been thought to take place by DNB, i.e. departure in boiling state from nucleate boiling. Several mechanisms to reach the DNB were suggested. Hewitt (1978) has presented the three most commonly postulated mechanisms as follows:

(a) A crowded bubble layer formed on the heated surface prevents to supply the heated surface with liquid, so that the film boiling takes place (Tong 1965).

(b) Local overheating at a dry patch generated by microlayer evaporation underneath a growing bubble.

(c) The wall temperature rise following the evaporation of liquid layer underneath vapor slugs or clots.

Kutateladze & Leontév (1966) and Tong (1968) have proposed a boundary layer separation model associated with an increase in vapor bubble generation.

On the other hand, Fiori & Bergles (1970) observed that active nucleate boiling took place in the liquid film existing under the vapor plug which was generated near the heating section outlet with increasing heat flux, and suggested that the DNB was resulted from the periodical wall temperature rise following liquid film disruption caused by the nucleate boiling. Molen & Galjee (1978) observed that the flow state at the DNB point was bubbly flow for a wide flow passage and slug flow for a narrow one, and found that the wall temperature under a vapor bubble or a vapor plug was able to exceed the rewetting temperature for water when the vapor phase stayed on the heated surface for about 0.1 s.

At the present time, as mentioned above, there is considerable uncertainty as to the DNB mechanism. Further study on the flow state of vapor and liquid adjacent to the heated surface with high heat fluxes is necessary to make clear the process leading to the DNB.

2. APPARATUS AND PROCEDURE

2.1 *Apparatus*

The flow system of the apparatus is the same as that shown in part I. The test section is a vertically arranged concentric annulus of 800 mm long, and R-113 liquid flows upwards in the annular passage as shown in figure 1. The inner tube is composed of a heating section, a stainless-steel tube of 8 mm o.d., 0.5 mm thick and 400 mm long, and copper electrodes silver soldered on both ends of the heating section. The heating section was heated uniformly by passing an alternating current through it. The outer tube is a polycarbonade pipe of 18 mm i.d., so that the hydraulic diameter D_e is 10 mm. The length of the entrance region to the heating section is 330 mm. In this experiment, a chromel–constantan thermocouple of 20 μm o.d. was inserted into the flow passage at the axial positions of 150, 250 and 350 mm from the heating section inlet (z/D_e = 15, 25 and 35). The microthermocouple probe assembly is also shown in figure 1. For traversing the microthermocouple toward the radial direction, a method was used to drive a support tube containing the microthermocouple by a micrometer. Experiments were performed for mass velocities G = 514 and 1239 kg/m^2 s and inlet liquid subcoolings ΔT_{sub} = 10, 20 and 30 K, under a constant inlet pressure p_{in} = 0.147 MPa.

2.2 *Temperature measurements and data processing*

For measuring the fluid temperature in the subcooled boiling flow, a method was used to record the microthermocouple output through an analog operational circuit which compen-

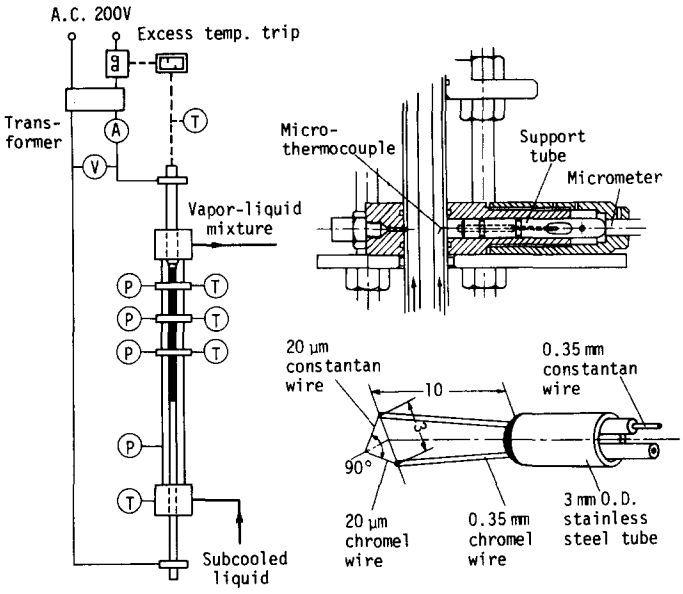

Figure 1. Test section and microthermocouple probe.

sates the time constant of the microthermocouple to enable the recording to follow the temperature fluctuation sufficiently. This method had been applied to an investigation on combustion fields by Tanaka & Shimamoto (1979). The compensation circuit used in this experiment was, similar to the Tanaka & Shimamoto's circuit, composed of an amplifier, a low pass filter (cutoff frequency was 2 kHz), an inverter circuit, a differential circuit and an addition circuit as shown in figure 2. Denoting the microthermocouple temperature and the environmental liquid temperature as T and T_f, a heat balance around the thermocouple wire is expressed as follows:

$$M\frac{\mathrm{d}T}{\mathrm{d}\tau} = T_f - T, \quad M = \frac{r_t c_{pt} \rho_t}{2h}, \tag{1}$$

where M is the time constant of the microthermocouple, r_t, c_{pt} and ρ_t are radius, specific heat and density of the thermocouple wire, and h represents the liquid phase heat transfer coefficient around the thermocouple wire. Then,

$$T_f = M\frac{\mathrm{d}T}{\mathrm{d}\tau} + T$$

and

$$E_f = M\frac{\mathrm{d}E}{\mathrm{d}\tau} + E, \tag{2}$$

where E and E_f are electromotive forces of the thermocouple corresponding to T and T_f,

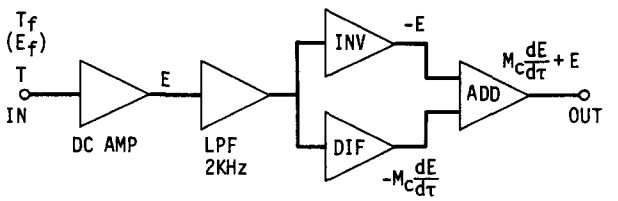

Figure 2. Block diagram of compensation circuit.

respectively. Therefore, the microthermocouple signal taken through the compensation circuit can follow the environmental liquid temperature fluctuation when the time constant of the differential circuit M_c shown in figure 2 is adjusted to coincide with the time constant of the microthermocouple M.

In actual measurements, the time constant of the differential circuit M_c was adjusted to be M by controlling the value M_c to eliminate overshoots which may appear on the output signal fluctuation. This adjustment was made for every position of the microthermocouple junction. The output signal from the compensation circuit was recorded on an analog data recorder and was analyzed by a digital computor. The sampling rate of A/D conversion was selected to be 1 ms for mass velocity $G = 514$ kg/m^2 s and 0.6 ms for $G = 1239$ kg/m^2 s.

Figure 3 shows a typical output signal fluctuation detected in the subcooled boiling flow field. The vapor bubble in the subcooled liquid is surrounded by a high temperature liquid layer, and the output signal can follow the sharp temperature variation in the liquid layer. This liquid layer seems to be considerably thin in consequence of the sharp response appeared in the recorded output signal. Therefore, the bubble frequency in the subcooled boiling flow and approximate periods of bubbles and liquid slugs passing at the microthermocouple point can be obtained from the recorded output signal fluctuation.

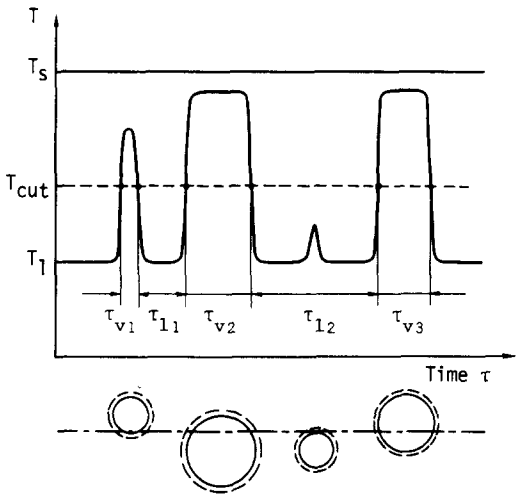

Figure 3. Temperature fluctuation detected in subcooled boiling field.

3. EXPERIMENTAL RESULTS AND DISCUSSION

3.1 *Boiling curve*

Figure 4 shows boiling curves obtained at $z/D_e = 35$, where the heat flux q is plotted against the wall superheat $\Delta T_s = T_w - T_s$. Arrows drawn in this figure indicate values of the CHF obtained for inlet liquid subcooling $\Delta T_{sub} = 10$, 20 and 30 K, respectively. The CHF in this paper is defined as the heat flux at which the power trip set at 380 K was actuated by the wall temperature detected at 10 mm upstream of the heating section outlet. The curves of q_{con} in this figure show the heat flux for forced convective liquid flow calculated from [2] in the part 1, and the line q_{bo} represents the heat flux for the fully developed pool boiling obtained from Rohsenow's equation (1952), i.e. [5] in the part 1.

3.2 *Distributions of time averaged temperature and relative intensity of temperature fluctuation*

Figure 5 shows the measured profiles of time averaged temperature $\overline{T}$ and relative intensity of the temperature fluctuation $\sqrt{(T')^2}/(T_w - T_L)$ in the cross section at $z/D_e = 0.35$. $\sqrt{(T')^2}$ is the rms value of the temperature fluctuation, T_w and T_L are the wall and bulk

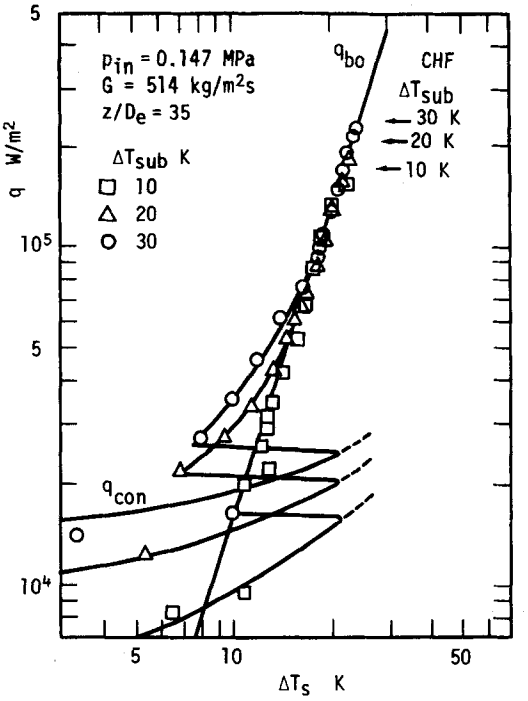

Figure 4. Boiling curves.

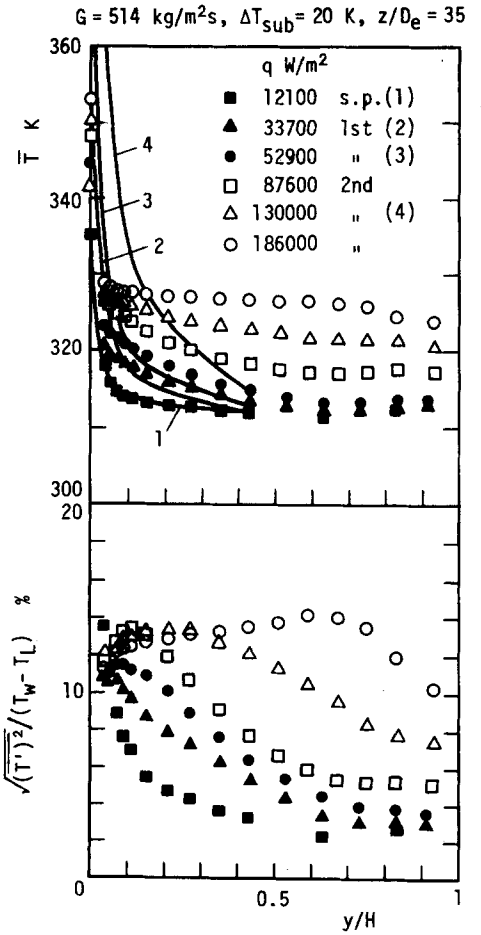

Figure 5. Profiles of time averaged temperature and relative intensity of the temperature fluctuation.

mean liquid temperatures, y is the distance from the heated surface, and H denotes the annular flow passage width (=5 mm). The letter symbols s.p., 1st and 2nd written in this figure indicate the flow state being in the single phase, the region I and region II of subcooled boiling flow, respectively. The saturation temperature T_s is 330 K in this condition. The solid lines drawn in this figure represent the universal temperature profiles for the single-phase turbulent flow which were calculated from the wall temperature derived by [2] in the part 1 and the following inner tube wall shear stress:

$$\tau_{wl} = \frac{(r_c^2 - r_1^2)}{2r_1} 4f \frac{1}{D_e} \frac{G^2}{2\rho_L}. \quad [3]$$

In this equation, f denotes the friction factor determined experimentally, [11] in the part 1, r_1 and r_c are the inner radius and the radius at zero shear stress in the annular passage. The value r_c was calculated from the following equation (Kays & Leung 1963):

$$\frac{r_c}{r_1} = \frac{1 + (r_2/r_1)^{1-n}}{1 + (r_2/r_1)^{-n}}, \quad n = 0.343, \quad [4]$$

where r_2 is the outer radius of the annular passage.

The experimental result for the single-phase flow is well agreed with the universal temperature profile. However, the fluid temperatures obtained for the subcooled boiling flow are lower than the universal profiles in a range nearby the heated surface, and the temperature gradients are considerably lower than those of the calculated profile even in the high subcooling region (region I), where the vapor bubble is not involved excepting on the heated surface. The temperature gradient in the single-phase turbulent flow depends mainly on the eddy diffusivity for heat ϵ_h and is expressed as follows:

$$\frac{dT}{dy} = \frac{q}{\rho_L c_{pL}(\nu_L/Pr_L + \epsilon_h)}. \quad [5]$$

Therefore, the above result suggests that the eddy diffusivity for heat ϵ_h in the subcooled boiling flow is generally large, and the turbulent heat diffusion is considered to be more active than that in the single-phase liquid flow.

The relative intensity of the temperature fluctuation is closely related to the vapor bubble density flowing there. As is seen in figure 5, the peak point of the relative intensity locates near the heated surface in the region I, and tends to go away from the heated surface in the region II where the vapor bubbles depart from the heated surface and disperse in the liquid core.

3.3 *Power spectrum*

Figure 6 shows power spectra of the temperature fluctuation obtained at several distances from the heated surface. The top of this figure shows the power spectra for the single-phase liquid flow, and the bottom shows that for the subcooled boiling flow of a low heat flux immediately after the incipient boiling where only few vapor bubbles exist on the heated surface. The latter result was obtained from the experimental data itself which may include the vapor bubble components. However, since the period of the microthermocouple being in the vapor bubbles is very short comparing with the total record time, this result can be considered to express the temperature fluctuation characteristics of the liquid phase. The boundaries of the viscous sublayer and the transition region for the single-phase liquid flow, $y^+ = 5$ and 30, are equivalent to $y/H = 0.02$ and 0.13, respectively. In this figure, the power spectrum function $G(f) \propto f^{-5/3}$ for the inertial subrange is drawn by a broken line for reference.

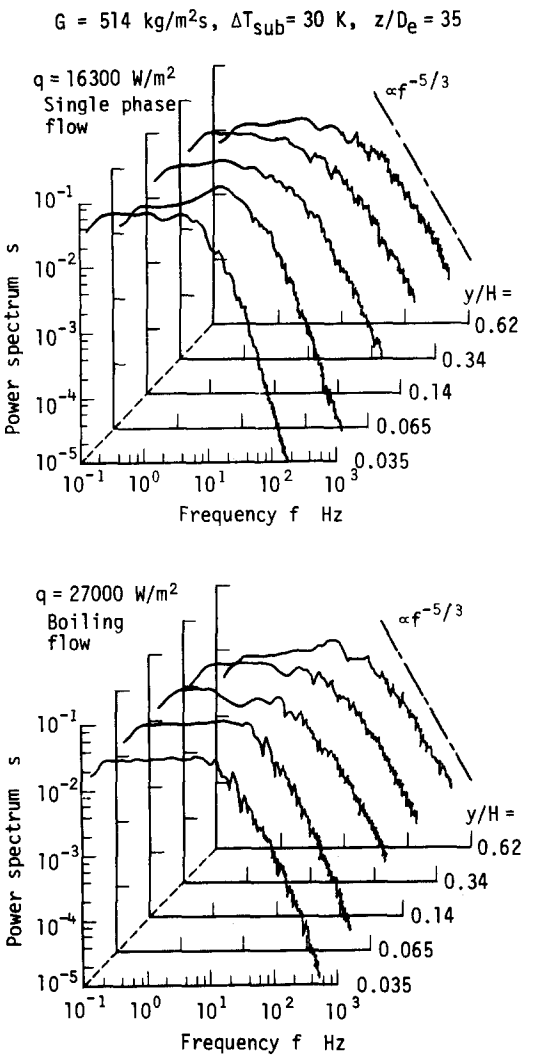

Figure 6. Power spectra of the temperature fluctuation.

In the single-phase liquid flow, the power spectrum follows to the $-5/3$ power in the turbulent region and tends to deviate as the location approaches to the heated surface with a decrease in high frequency components. In the boiling flow, however, the high frequency components are increased in the whole range and the $-5/3$ power spectrum is maintained even in a range adjacent to the heated surface. This result also suggests that the turbulent heat diffusion in the liquid phase is more active in the boiling flow than that in the single-phase liquid flow.

3.4 *Probability density distribution of fluid temperature*

The probability density distributions of the fluid temperature at various distances from the heated surface and at various heat fluxes were derived by the recorded data processing. Figure 7 shows an example of the results obtained at the condition of $G = 514$ kg/m^2 s and $\Delta T_{sub} = 20$ K, in which figure (a) represents the distributions for the single-phase liquid flow state, figure (b) the state of region I of subcooled boiling flow, and figure (c) the high heat flux state of region II. In the region I, the high temperature components become dominant in the range nearby the heated surface in comparison with the single-phase liquid flow state. Photographic observation of the boiling behaviour has shown that a dense bubbly layer begins to form on the heated surface at this heat flux. The above trend in the region I seems to be caused by the bubbly layer formation. As the heat flux is increased and the state enters

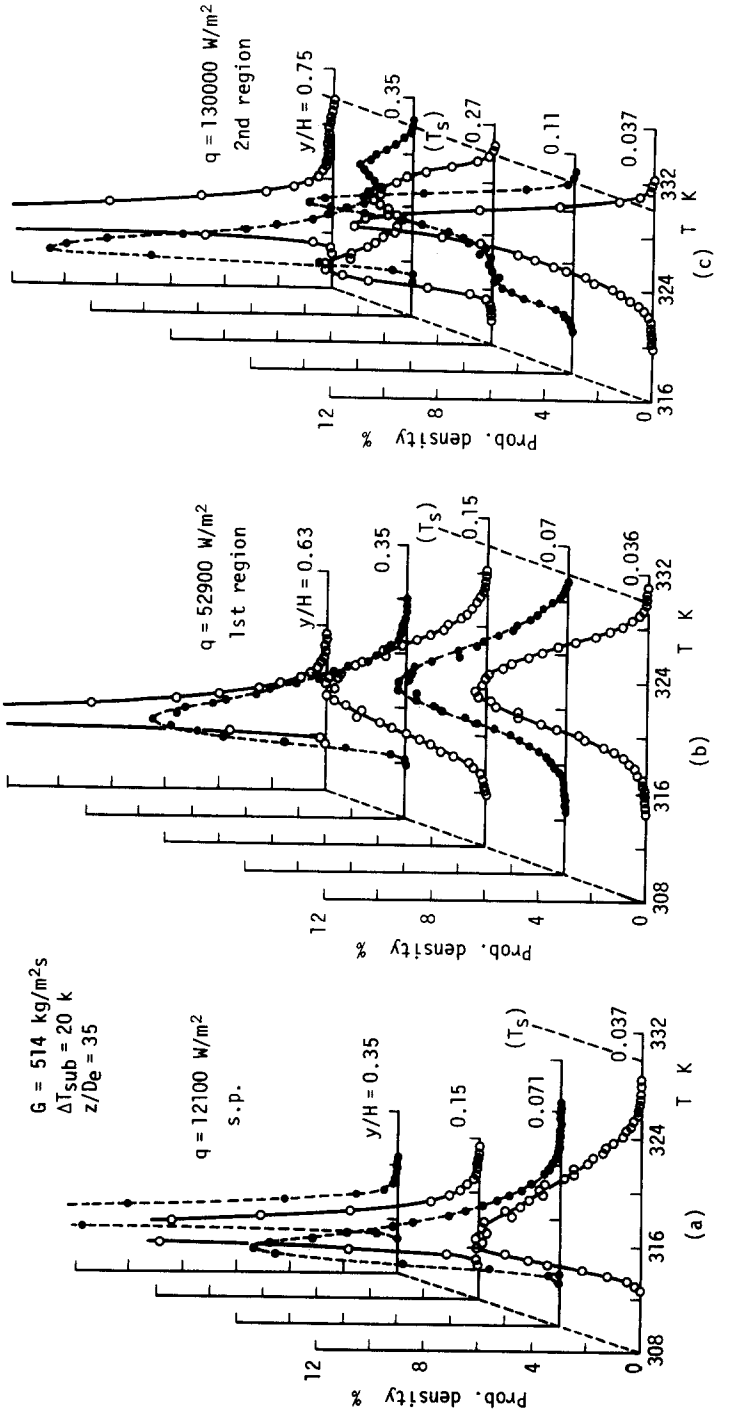

Figure 7. Probability density distributions of the fluid temperature (effect of heat flux).

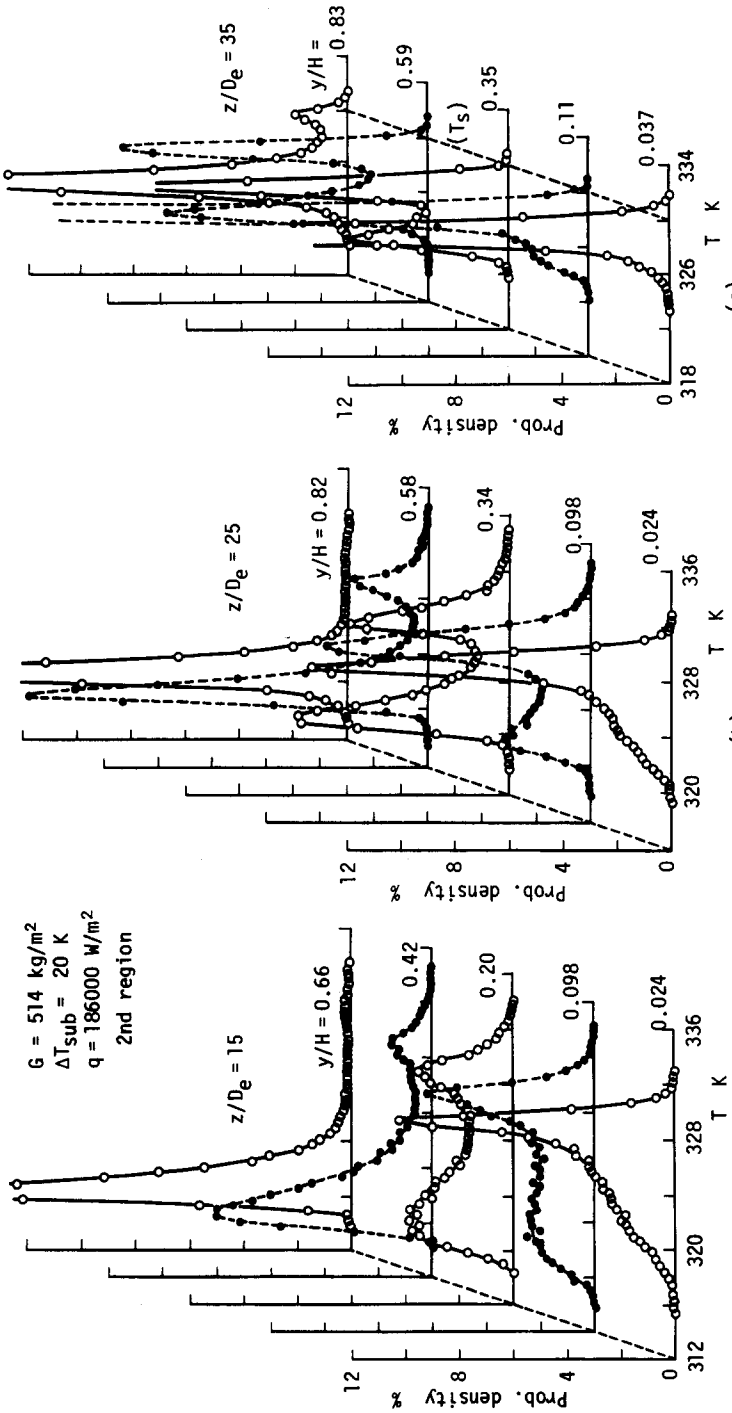

Figure 8. Probability density distributions of the fluid temperature (variation along heated length).

into the region II, the high temperature components increase further and two peaks, one is on a low temperature side and the other on a high temperature side, appear at the locations far from the heated surface, as is seen in figure (c). The peak on a high temperature side represents arrival of the bubbles departed from the heated surface. At the locations adjacent to the heated surface, the low temperature components decrease with increasing heat flux, and the peak on a low temperature side disappears.

Figure 8 shows the probability density distributions of the fluid temperature at z/D_e = 15, 25 and 35 for a higher heat flux close to the CHF. The result indicates the high temperature components develop along the heated surface. At z/D_e = 35 near the heating section outlet, the low temperature components at locations adjacent to the heated surface decrease and the width of the temperature fluctuation becomes narrow remarkably.

3.5 *Distribution of bubble frequency and frequencies of vapor and liquid periods*

In order to investigate the flow characteristics of the subcooled boiling, the frequencies of the temperature fluctuation signal across a certain temperature level T_{cut} and of the period in which the signal is over T_{cut} were counted. Here, the temperature at the bottom between the two peaks observed in the above probability density distributions of the fluid temperature was adopted as T_{cut}. As is seen in figure 3, the components of higher temperature than T_{cut} were regarded approximately as the vapor phase, and others were regarded as the liquid phase. The bubble frequency and the frequencies of vapor phase period τ_v and liquid phase period τ_l were derived utilizing the program developed by Ohsaki (1976) for analyzing the earthquake waves.

Figure 9 shows the profiles of bubble number N detected across the flow passage at z/D_e = 35. In this case, T_{cut} is 326.6 K for G = 514 kg/m^{2}s and 325.1 K for 1239 kg/m^2 s. The vapor bubbles are restrained near the heated surface in the region I. In the region II, the profile developes to a shape of a peak at the location close to the heated surface, and then another peak appears far from the heated surface as the heat flux is increased. Such bubble frequency distributions as those in the region II have been observed by Sekoguchi *et al.* (1976) in their experiment for the air–water two phase flow arranged to simulate the flow boiling. According to the photographic observation mentioned in the part I, this case is in a

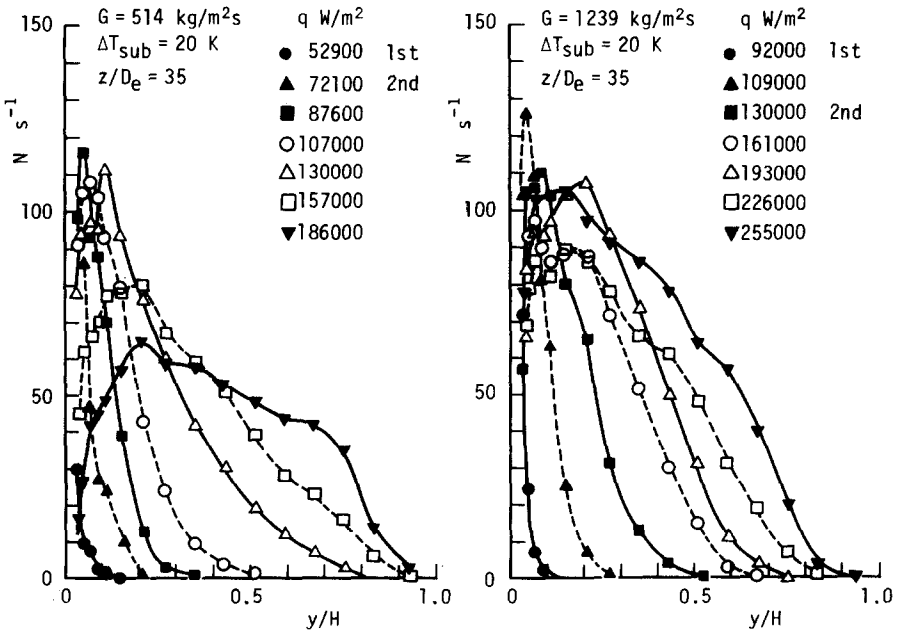

Figure 9. Profiles of bubble frequency.

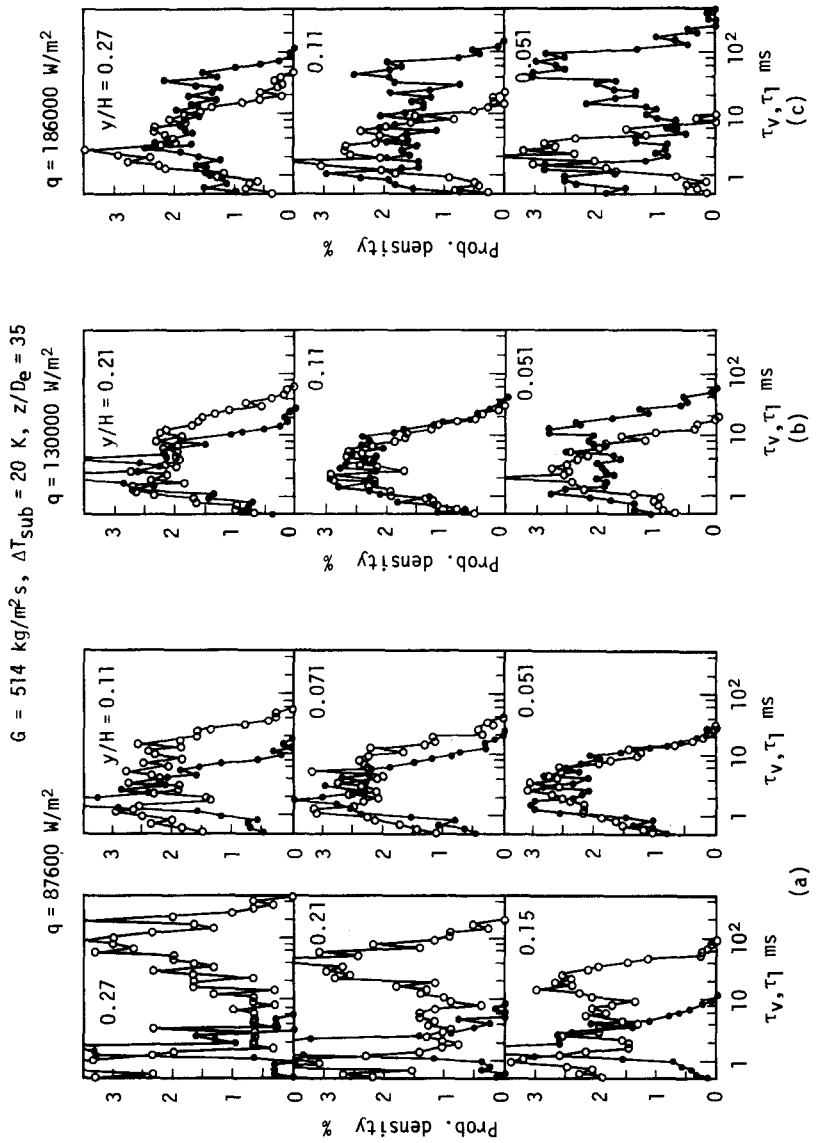

Figure 10. Probability density distributions of vapor and liquid periods (effect of heat flux).

state where the vapor bubbles are departing from the developed bubbly layer to the liquid core. The peak nearby the heated surface represents the center of the bubbly layer formed on the heated surface, and the other peak far from the heated surface shows that the departed bubbles are crowded around the location of this peak. However, it should be noted that increasing the heat flux close to the CHF, the bubble frequency in a range adjacent to the heated surface decreases sharply and the peak nearby the heated surface disappears.

Figure 10 shows the frequency distributions of vapor and liquid periods obtained at $z/D_e = 35$ under a condition of $G = 514$ kg/m^2 s and $\Delta T_{sub} = 20$ K. The solid symbols ● in this figure represent the vapor period and the open symbols ○ the liquid period. Long period components of the liquid phase decrease as the location approaches to the heated surface, and those of the vapor phase increase remarkably with increasing heat flux. Here, the long period components are noted to comprehend the whole situation of the flow characteristics. For this purpose, the probability density is plotted against to each class of the period which was chosen to be wide in proportion to its period. Since the period of vapor phase in this figure is derived by assuming the components of higher temperature than T_{cut} being the vapor phase, as mentioned before, the vapor period shown may be a little longer than the actual vapor period. However, it is possible to understand the effect of heat flux on the vapor period from this figure. Figure 11 shows the axial variation of the periods at a high heat flux $q = 1.86 \times 10^5$ W/m^2. Advancing to the heating section outlet, the liquid period at the locations adjacent to the heated surface decreases and the vapor components of remarkably long periods are developed there.

When the heat flux is raised near the CHF, very long period components of the vapor phase appear in the downstream part of the heating section, together with a sharp decrease in the bubble fequency. This fact suggests that large volume bubbles yielded by coalescence of bubbles flow periodically close to the heated surface. Figure 12 shows the relation between the maximum value of the vapor period $(\tau_v)_{max}$ and the heat flux at a location adjacent to the heated surface $y/H \fallingdotseq 0.05$ ($y \fallingdotseq 0.25$ mm). Arrows drawn in this figure represent the CHF. As is seen in this figure, a small increment of heat flux causes a remarkable increase in $(\tau_v)_{max}$ when the heat flux is elevated near the CHF. This trend of $(\tau_v)_{max}$ is considered to be related closely to the occurrence of the CHF condition.

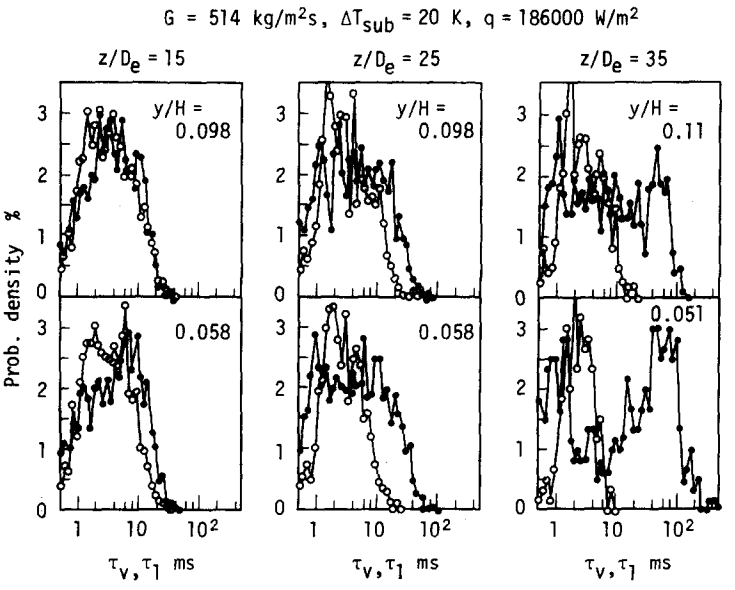

Figure 11. Probability density distributions of vapor and liquid periods (variation along heated length).

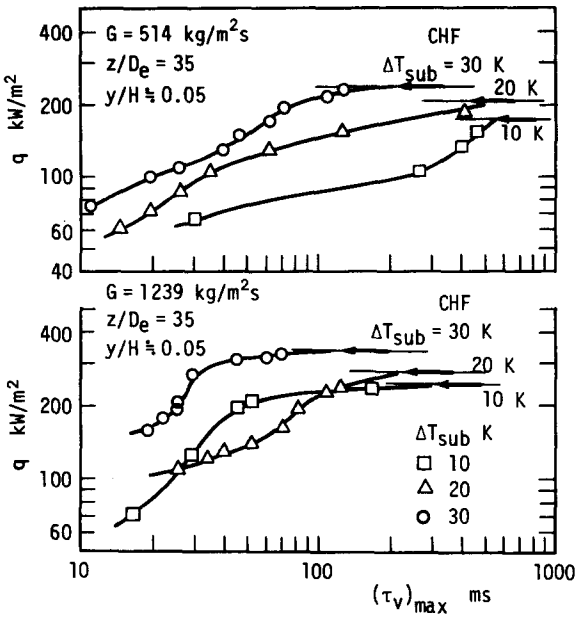

Figure 12. Variations of the maximum vapor period.

A thin liquid layer with nucleate boiling has been considered to exist underneath the large coalescent bubble. Katto *et al.* (1971, 1980) have observed a thin liquid layer with nucleate boiling by high heat flux experiments for saturated pool boiling and for saturated boiling in a liquid flow parallel to the heated surface. However, when the passing period of the coalescent bubbles becomes long as mentioned above, a part of the liquid layer underneath the coalescent bubble will dryout, and the wall temperature at the dry spot will begin to rise.

It seems to be difficult to estimate the time required for evaporating the thin liquid layer with nucleate boiling. Supposing a superheated liquid layer at the CHF q_{crit}, the thickness δ_c is given by

$$q_{crit} = k_L(\Delta T_s)_{crit}/\delta_c, \qquad [6]$$

and the evaporation time of this layer τ_0 can be expressed as

$$\tau_0 = \rho_L \delta_c H_{LG}/q_{crit}, \qquad [7]$$

where $(\Delta t T_s)_{crit}$ is the wall superheat at the CHF condition and H_{LG} denotes the latent heat of evaporation. The evaporation time τ_0 is less than 10 ms in this experimental condition. The actual evaporation time of the liquid layer may be longer than the above value, since an amount of liquid flows into the liquid layer. However, it seems to be that the actual evaporation time of the liquid layer is considerably shorter than the maximum period of the vapor phase shown in figure 12.

Provided the added heat flux q is used entirely to rise the wall temperature at the dry spot, the relation between the wall temperature rise ΔT_w and the heating time τ_h is expressed as follows:

$$\tau_h = \rho_w c_{pw} \delta_s \Delta T_w/q, \qquad [8]$$

where ρ_w and c_{pw} are the density and specific heat of the heated wall, and δ_s is the wall

Table 1. The CHF condition and the heating times required for given wall temperature rises

G	ΔT_{sub}	q_{crit}	$(\Delta T_s)_{crit}$	τ_h ms		
kg/m^{2}s	K	kW/m^2	K	ΔT_w = 20 K	30 K	110 K
514	30	241	24.2	141	211	775
	20	211	23.1	161	241	885
	10	174	21.7	194	292	1069
1239	30	332	26.9	102	153	561
	20	277	25.3	122	183	673
	10	244	24.3	139	208	765

thickness. Table 1 shows the values of τ_h for given temperature rises ΔT_w = 20, 30 and 110 K calculated by substituting the CHF q_{crit} of this experiment into [8]. Ueda *et al.* (1983) have derived boiling curves experimentally for R-113 upflow and shown that the wall superheat ΔT_s at the onset of rewetting, i.e. the boundary between transition boiling and film boiling, for subcooled and low quality regions is in a range of 120–140 K. The wall temperature rise ΔT_w corresponding to the above superheats is about 110 K. The maximum vapor periods at the CHF shown in figure 12 correspond approximately to the heating times for ΔT_w = 30 K and are less than those for ΔT_w = 110 K. However, the temperature drop of the dry spot resulting from the quenching which is caused by a liquid slug following a coalescent bubble can not be so much. The passing period of the liquid slug is short at the CHF condition, and the quench rate of the dry spot at high wall superheats exceeding $(\Delta T_s)_{crit}$ does not seem to be so high. Therefore, the large wall temperature rise associated with the CHF in this experiment is considered to be caused by periodical heating of the wall, repetition of an overheating of the dry spot during a long vapor period and a less cooling during the following liquid period, to the rewetting temperature and a subsequent sharp temperature rise under film boiling.

4. CONCLUSIONS

The measurements of local temperature fluctuation were performed by means of a microthermocouple on the R-113 upward subcooled boiling flow in an annulus with a uniformly heated inner tube. From the results, the following conclusions were obtained.

(1) The experimental results on the time averaged temperature distribution and the power spectrum of the temperature fluctuation suggest that the turbulent heat diffusion is more active in the subcooled boiling flow than that in the single-phase liquid flow.

(2) Increasing the heat flux near the CHF, the bubble frequency in a range adjacent to the heated surface decreases, and long period components of the vapor phase are developed. This result shows that large coalescent bubbles appear periodically close to the heated surface.

(3) The maximum vapor period increases remarkably with a small increment of heat flux in the high heat flux conditions close to the CHF.

(4) Within the passing period of a coalescent bubble mentioned above, a part of the liquid layer existing underneath the coalescent bubble can evaporate and cause some wall temperature rise at the dry spot. It seems to be that the large wall temperature rise associated with the DNB in this experiment is resulting from periodical overheating of the wall to the rewetting temperature and a subsequent sharp temperature rise under film boiling.

Acknowledgement—The authors gratefully acknowledge the support for this work by the research fund (Grant in Aid of Energy Special Project Research) of the Ministry of Education, Japan.

REFERENCES

AFGAN, N. 1975 Boiling liquid superheat. *Adv. Heat Transfer,* **11,** 1–49.

AKIYAMA, M. & TACHIBANA, F. 1974 Motion of vapor bubbles in subcooled heated channel. Bull. Jpn. Soc. Mech. Engr. **17,** 241–247.

DELHAYE, J. M., SEMERIA, R. & FLAMAND, J. C. 1973 Void fraction and vapor and liquid temperatures: Local measurements in two-phase flow using a microthermocouple. *Trans. ASME, Ser. C* **95,** 365–370.

FIORI, M. P. & BERGLES, A. E. 1970 Model of critical heat flux in subcooled flow boiling. *4th Int. Heat Transfer Conf.,* Paris **6,** B6.3.

HEWITT, G. F. 1978 Critical heat flux in flow boiling. *Proc. 6th Int. Heat Transfer Conf., Toronto* **6,** 143–171.

HINO, R. & UEDA, T. 1985 Studies on heat transfer and flow characteristics in subcooled flow boiling (Part I, Boiling characteristics). *Int. J. Multiphase Flow* **11,** 269–281.

JIJI, L. M. & CLARK, J. A. 1964 Bubble boundary layer and temperature profiles for forced convection boiling in channel flow. *Trans. ASME,* Ser. C **86,** 50–58.

KATTO, Y. & YOKOYA, S. 1971 Mechanism of boiling crisis and transition boiling in pool boiling. *Trans. Jpn. Soc. Mech. Engr.* **37,** 535–545.

KATTO, Y. & KURATA, C. 1980 Critical heat flux of saturated convective boiling on uniformly heated plates in a parallel flow. *Int. J. Multiphase Flow* **6,** 575–582.

KAYS, W. M. & LEUNG, E. Y. 1963 Heat transfer in annular passages—hydrodynamically developed turbulent flow with arbitrarily prescribed heat flux. *Int. J. Heat Mass Transfer* **6,** 537–557.

KUTATELADZE, S. S. & LEONTÉV, A. I. 1966 Some applications of the asymptotic theory of the turbulent boundary layer. *Proc. 3rd Int. Heat Transfer Conf., Chicago* **3,** 1–6.

OHSAKI, Y. 1976 *Fundamentals to Spectral Analysis for Earthquake.* 17–34, Kajima Press, Japan.

ROHSENOW, W. M. 1952 A method of correlating heat-transfer data for surface boiling of liquids. *Trans. ASME* **74,** 969–976.

SEKOGUCHI, K., NISHIKAWA, K., NAKASATOMI, M., HIRATA, N. & HIGUCHI, H. 1974 Flow boiling in subcooled and low quality regions—heat transfer and local void fraction. *Proc. 5th Int. Heat Transfer Conf., Tokyo* **4,** 180–184.

SEKOGUCHI, K., KAWAKAMI, Y. & NISHIKAWA, K. 1976 Flow simulation of forced-flow boiling with air–water two-phase fluids (1st Report, On the distribution of bubbles). *Bull. Jpn. Soc. Mech. Engr.* **19,** 187–194.

SEKOGUCHI, K., TANAKA, O., ESAKI, S. & IMASAKA, T. 1980 Prediction of void fraction in subcooled and low quality boiling regions. *Bull. Jpn. Soc. Mech. Engr.* **23,** 1475–1482.

TANAKA, Y. & SHIMAMOTO, Y. 1979 Simultaneous measurement of fluctuating temperature and velocity in a combustion field. *Bull. Jpn. Soc. Mech. Engr.* **22,** 390–397.

TONG, L. S. 1965 Boiling Heat Transfer and Two-Phase Flow. 140–145, John Wiley & Sons, New York.

TONG, L. S. 1968 Boundary-layer analysis of the flow boiling crisis. *Int. J. Heat Mass Transfer* **11,** 1208–1211.

UEDA, T., TSUNENARI, S. & KOYANAGI, M. 1983 An investigation of critical heat flux and surface rewet in flow boiling systems. *Int. J. Heat Mass Transfer* **26,** 1189–1198.

VAN DER MOLEN, S. B. & GALJEE, F. W. B. M. 1978 The boiling mechanism during burnout phenomena in subcooled two-phase water flows. *Proc. 6th Int. Heat Transfer Conf., Toronto* **1,** 381–385.

WALMET, G. E. & STAUB, F. W. 1969 Pressure, temperature and void fraction measurement in nonequilibrium two-phase flow. *11th ASME Heat Transfer Conf., Two-Phase Flow Instrumentation,* 89–101.